The pH-dependent tertiary structure of a designed helix–loop–helix dimer

Gunnar T Dolphin and Lars Baltzer

Background: *De novo* designed helix–loop–helix motifs can fold into well-defined tertiary structures if residues or groups of residues are incorporated at the helix–helix boundary to form helix-recognition sites that restrict the conformational degrees of freedom of the helical segments. Understanding the relationship between structure and function of conformational constraints therefore forms the basis for the engineering of non-natural proteins. This paper describes the design of an interhelical $HisH^+$–Asp^- hydrogen-bonded ion pair and the conformational stability of the folded helix–loop–helix motif.

Results: GTD-C, a polypeptide with 43 amino acid residues, has been designed to fold into a hairpin helix–loop–helix motif that can dimerise to form a four-helix bundle. The folded motif is in slow conformational exchange on the NMR timescale and has a well-dispersed ^{1}H NMR spectrum, a narrow temperature interval for thermal denaturation and a near-UV CD spectrum with some fine structure. The conformational stability is pH dependent with an optimum that corresponds to the pH for maximum formation of a hydrogen-bonded ion pair between $HisH17^+$ in helix I and $Asp27^-$ in helix II.

Conclusions: The formation of an interhelical salt bridge is strongly suggested by the pH dependence of a number of spectroscopic probes to generate a well-defined tertiary structure in a designed helix–loop–helix motif. The thermodynamic stability of the folded motif is not increased by the formation of the salt bridge, but neighbouring conformations are destabilised. The use of this novel design principle in combination with hydrophobic interactions that provide sufficient binding energy in the folded structure should be of general use in *de novo* design of native-like proteins.

Address: Department of Chemistry, Göteborg University, 412 96 Göteborg, Sweden.

Correspondence: Lars Baltzer
E-mail: baltzer@oc.chalmers.se

Key words: *De novo* design, helix–loop–helix, salt bridge, tertiary structure

Received: **03 April 1997**
Revisions requested: **24 April 1997**
Revisions received: **16 July 1997**
Accepted: **22 July 1997**

Published: **22 September 1997**
http://biomednet.com/elecref/1359027800200295

Folding & Design 22 September 1997, **2**:319–330

Introduction

The *de novo* design of proteins [1] that fold into well-defined tertiary structures tests our understanding of the folding problem and has important applications in the engineering of, for example, novel catalysts [2], immunogenic folds [3] and cofactor-linked proteins [4]. The design principles have proven to be elusive, however, since the overwhelming majority of *de novo* designed proteins are best described as molten globules. The discrimination between so-called native-like proteins and molten globule structures [5] is based on characteristics such as the appearance of the ^{1}H NMR spectrum, amide proton exchange rates, the thermal melting point and the binding of the dye 8-anilino-1-naphthalenesulphonic acid (ANS). So far, only two designed four-helix bundles, α_2D [6] and GTD-43 [7,8], and a small number of other folds [9,10] have been reported to fulfill some of these criteria and the key problem has been the engineering of the hydrophobic core. Until recently, the most common strategy in the pursuit of well-packed interiors was the design of shape-complementary hydrophobic interfaces between amphiphilic helices. The lack of progress despite much effort led Handel *et al.* [11] to propose that shape complementarity alone was not enough and that the incorporation of conformational constraints was necessary to achieve ordered hydrophobic cores and well-defined tertiary structures. The design of α_2D was based partly on the expected ability of charged sidechains on each side of the hydrophobic ridge to limit the mobility of the helical segments.

We reported recently on the four-helix bundle GTD-43 [7,8], which is in slow conformational exchange on the NMR timescale and has a well-dispersed ^{1}H NMR spectrum, slow amide proton exchange rates and a narrow temperature interval for thermal denaturation. The aromatic residues Phe10, Trp13 and Phe34 were designed to form an aromatic ensemble that could restrict the dynamics of the hydrophobic residues in the folded structure. It was shown by NMR spectroscopy that the aromatic ensemble did in fact form and that the aromatic residues form a conformational constraint [8]. The designed structure of GTD-43 also contained an interhelical salt bridge between His17 and Asp27 located at the hydrophobic core–loop boundary, but due to the poor solubility of

GTD-43 above pH 4, the function of the designed salt bridge could not be investigated spectroscopically.

Internal salt bridges are found in native proteins and were previously believed to stabilise the tertiary structure because large binding energies are expected from interactions between charged residues in environments with low dielectric constants. The replacement of a buried salt bridge triad by complementary hydrophobic residues was, however, reported to result in a functional protein that was more stable than the native one [12]. The introduction of buried salt bridges in *de novo* designed proteins has not so far been successful, but the engineering of an internal salt bridge in the GCN4 coiled-coil dimer was recently found to introduce specificity and helix–helix recognition, although no net increase in binding energy was obtained [13].

GTD-43 has now been modified in three positions to form GTD-C, a polypeptide that is sufficiently soluble to allow studies over a wide temperature and pH range, and in order to assess the importance of the hydrogen-bonded $HisH^+$–Asp^- ion pair, a number of spectroscopic measurements have been carried out as a function of pH. We now report that the optimum conformational stability of GTD-C correlates well with the expected formation of a salt bridge between His17 and Asp27. The results suggest that salt bridges may be of general use in combination with hydrophobic residues to engineer native-like properties in *de novo* designed proteins.

Results

The design of GTD-C

The design of GTD-C was based on the design and solution structure of GTD-43, a polypeptide with 43 amino acid residues that folds into a helix–loop–helix motif and dimerises to form a four-helix bundle [8]. The design of helices has been reviewed recently [1] and the generally accepted strategy was followed in the design of GTD-43 and GTD-C. In short, the helical sequences contain amino acid residues with helix propensity and the folded helices were stabilised by capping and dipole stabilising residues as well as by salt bridges. The loop sequence of GTD-43 and GTD-C is G-T-G-P (Figure 1). Complementary hydrophobic interfaces were engineered from Nval, Ile, Leu, Phe and Trp residues and the aromatic residues Phe10 and Trp13 in helix I and Phe34 in helix II were designed and shown by NMR spectroscopy to interact in the folded state. Unique conformational stability was induced by the aromatic ensemble and GTD-43 was characterised by a well-dispersed ^{1}H NMR spectrum that was in slow exchange on the NMR timescale, slow amide proton exchange rates in part of the sequence and a narrow temperature interval for thermal denaturation. However, GTD-43 was poorly soluble in the pH interval above 4 and spectroscopic investigations were inconclusive.

Figure 1

```
 1                                  17    20
S-L-E-A-Nva-L-Q-E-A-F-R-A-W-L-Q-Y-H-A-A-K-

                                    21    24
                                   -G-T-G-P-

  N-I-K-A-Nva-L-Q-K-A-F-A-H-L-A-E-Q-D-Q-A-
 43                                   27  25
```

The amino acid sequence of GTD-C presented using the one-letter code except for norvaline which is shown as Nva. His17 and Asp27 are the residues designed to form an interhelical salt bridge.

In order to increase the solubility without affecting the structural properties, two amino acid residues were replaced on the surface of the folded polypeptide. Arg32 was replaced by His and Aad36 (α-amino adipic acid) was replaced by Lys. The replacement of Aad3 by Glu3 is a very minor modification as its only effect is to decrease by one the number of methylene groups of the sidechain. The amino acid sequence of GTD-C is shown in Figure 1. The incorporation of His32 and Lys36 also had another purpose as they are known to form a site for the reaction with *p*-nitrophenyl esters. A histidine and a lysine residue in a helix conformation, four positions apart in the amino acid sequence, have previously been shown to react with *p*-nitrophenyl esters with increased rates of *p*-nitrophenol release over that of 4-methyl imidazole at pH 5.85 and 290K by factors of 5 to 35 depending on the solvent [14,15]. The incorporation of the two residues in GTD-C therefore represents the first step towards the development of catalytically active sites in designed polypeptides with well-defined tertiary structures.

The structure of GTD-C

The CD spectrum of GTD-C in aqueous solution at pH 4.8 and ambient temperature is characteristic of an α-helical protein with minima at 222 nm and 208 nm and a maximum at 195 nm. The mean residue ellipticity at 222 nm, θ_{222}, is $-20{,}500 \pm 1000$ deg cm^2 dmol^{-1}, which is the same, within experimental error, as that reported for GTD-43 and the small modifications introduced into the sequence of GTD-C apparently do not much affect the tertiary structure. The mean residue ellipticity of GTD-C, and the ratio of mean residue ellipticities $\theta_{222}/\theta_{208}$, is independent of concentration in the range 3.8 to 760 μM in 50 mM phosphate buffer at pH 5.8 and 298K. The mean residue ellipticity of GTD-43 is also independent of concentration and GTD-43 has previously been shown by ultracentrifugation to fold into a dimer.

The mean residue ellipticity at 222 nm is pH dependent in the range pH 2 to pH 8.5 (Figure 2). At pH 2, θ_{222} is only $-12{,}000$ deg cm^2 dmol^{-1}, but the helical content

Figure 2

The CD spectrum of GTD-C at 61 μM peptide concentration and 298K as a function of pH. **(a)** An isodichroic point is observed near 203 nm suggesting that pH denaturation can be described by a two-state model. **(b)** The mean residue ellipticity of GTD-C at 222 nm (filled circles) and the ratio of mean residue ellipticities of GTD-C at 222 and 208 nm (filled squares) as a function of pH.

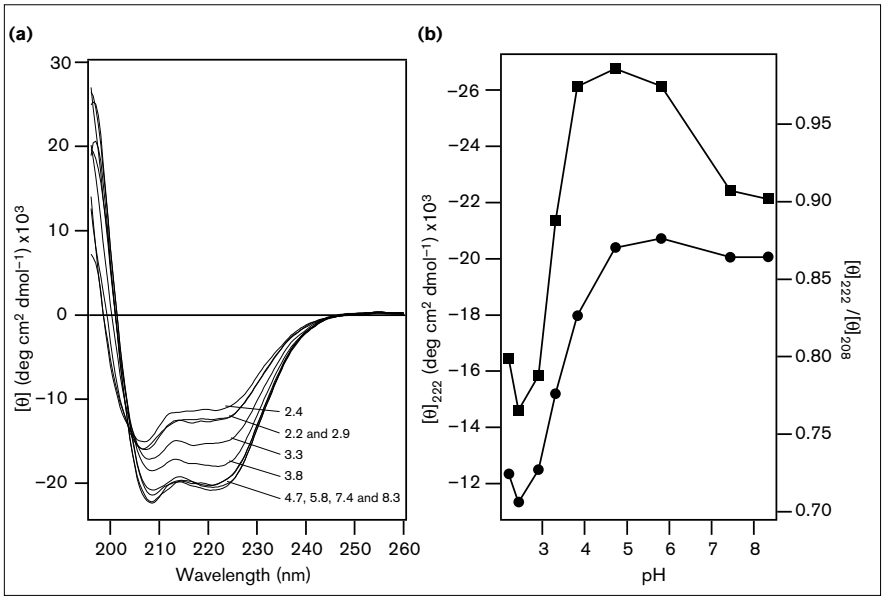

increases from pH 2.5 to reach its maximum value at pH 5.5 after which it decreases slightly above pH 6. The change at low pH follows approximately the deprotonation of carboxylic acids and is probably due to the formation of favourable ion pairs and neutralisation of repulsive charge–charge interactions. The slight increase in helicity at very low pH that is observed for GTD-C has been reported for a number of coiled-coil peptides and has been assigned to changes in helix propensity of the protonated acidic sidechains and increased hydrophobic interactions between the uncharged residues [16].

The ratio of mean residue ellipticities, $\theta_{222}/\theta_{208}$, is commonly interpreted in terms of the formation of coiled-coil motifs [17]. A ratio of 1 is considered to correspond to an α-helical coiled coil and a value of ~0.8 to a polypeptide with single-stranded helices. The magnitude of the ratio is also pH dependent and increases with pH from a value of less than 0.8 at pH 2.5 to a rather broad maximum with a value that is close to 1 and is centered around pH 5. The pH dependence of the ratio $\theta_{222}/\theta_{208}$ suggests an optimum for the supercoiling of GTD-C at pH 5.

The tryptophan fluorescence maximum at 341 nm in 50 mM phosphate buffer at pH 5.8 and 288K is blue shifted in comparison with that of the GuHCl denatured peptide at 360 nm, which shows that Trp13 is at least partly buried in the hydrophobic core of the folded structure [18]. The fluorescence intensity of the folded state of GTD-C at pH 5.8 is only 30% of that of the denatured state, probably due to quenching by the protonated form of His17. The imidazolium ion has been shown previously to quench Trp fluorescence [19]. The fluorescence intensity increased with pH and follows the depronation of a monobasic acid with a pKa of 6.5.

The conformational stability of GTD-C

The ^{1}H NMR spectrum of GTD-C in 90% H_2O/10% D_2O at pH 4.5 and 283K is well dispersed and its temperature dependence shows that GTD-C is in slow exchange on the NMR timescale (Figure 3). The chemical shift range of the amide protons is 2.3 ppm, which compares well with those of other designed proteins and is comparable to that of IL-4 (2.9 ppm) [20], a naturally occurring four-helix bundle. Similar comparisons can also be made for the methyl region and for the α proton region. The appearance of the ^{1}H NMR spectrum is pH dependent (Figure 4) and the best resolution is obtained between pH 4 and pH 5.

The thermal denaturation of GTD-C at pH 5.8 is monitored by recording the CD spectrum as a function of temperature (Figure 5). The decrease in $-\theta_{222}$ was masked by the precipitation of peptide and the adhesion of peptide to the glass wall of the cuvette. Above 358K, GTD-C precipitates irreversibly and a β-sheet is formed that cannot be removed from the cell window even after repeated rinsing with water and ethanol. A typical β-sheet CD spectrum remains and as a result no melting point is obtained from the temperature dependence of θ_{222}. The mean residue ellipticity at 208 nm, θ_{208}, was used instead as it is little affected by the spectrum of the glass-bound peptide. In the interval from 275K to 335K, the negative value of θ_{208} decreases by roughly 15%. Above 335K, there is a rapid decrease in the helical content with temperature and at 358K, θ_{208} is only –5000 deg cm^2 dmol^{-1}. Published values

Figure 3

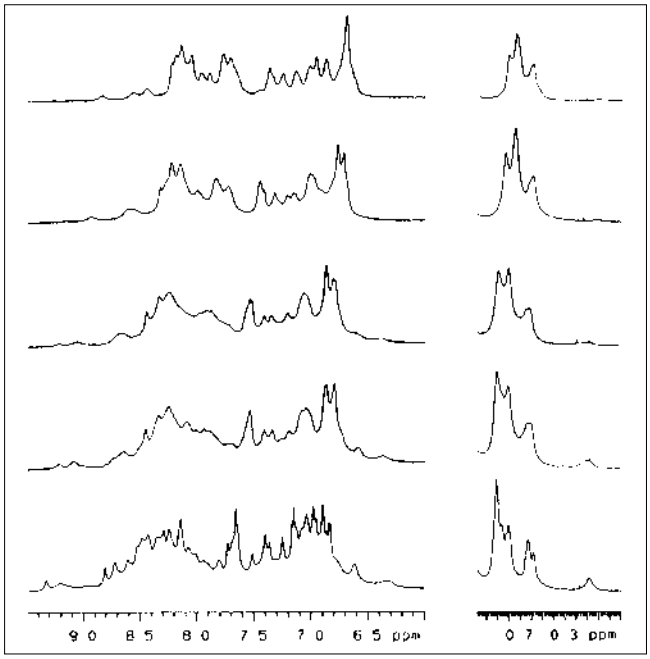

Parts of the 500 MHz ^{1}H NMR spectrum of GTD-C at a concentration of 210 μM and pH 4.4 as a function of temperature. From bottom to top, the temperatures are 283K, 298K, 303K, 313K and 323K. The resolution at 283K is dramatically better than that at elevated temperatures, which shows that as the conformational exchange processes are accelerated the resonances are broadened and at low temperature GTD-C approaches the slow exchange limit.

of the mean residue ellipticities of dissociated helix–loop–helix dimers are negative [3]. The thermal denaturation at the temperature for precipitation can therefore be assumed to be past its midpoint and the temperature interval for thermal denaturation is on the order of 30K. The observed isodichroic point near 203 nm suggests that the thermal denaturation may be described by a two-state helix-to-coil transition.

The near-UV CD spectrum of GTD-C (Figure 6) exhibits a strong broad signal between 250 and 310 nm, with some vibronic structure, which is typical of a tryptophan in an ordered environment [21]. The spectrum is dominated by the Trp ^1L_a and ^1L_b bands, the two broad positive ^1L_a CD bands extend from approximately 250 to 310 nm and the negative ^1L_b vibronic bands were identified at 293 and 285 nm from the 7 nm vibronic spacing found for tryptophan.

The ^1L_a and ^1L_b CD bands of Trp13 have different signs and vary independently of one another in intensity as a function of pH. The intensities of the broad ^1L_a bands vary with pH and have a maximum between pH 3.5 and 5, which supports the conclusion that the tertiary structure is best defined in that range, as the intensity is expected to

Figure 4

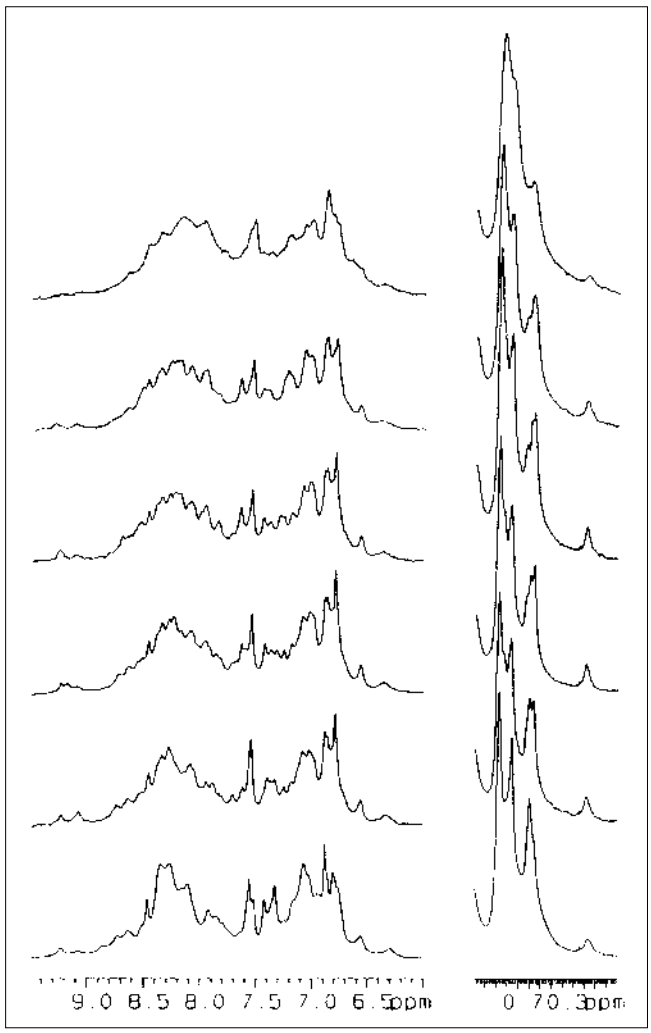

Parts of the 500 MHz ^{1}H NMR spectrum of GTD-C at a concentration of 190 μM and 293K as a function of pH. From bottom to top, the pH values are 3.0, 4.0, 4.5, 4.9, 5.5 and 6.3. The resolution at pH 4.5 and at pH 4.9 is considerably better than at pH 3.0 and pH 6.3, where the spectrum shows broadened resonances and poor resolution, which is typical of molten globule structures.

decrease with increasing mobility of the sidechains. The intensity of the weak and negative ^1L_b vibronic band of Trp13 at 293 nm becomes more negative with pH, and through curve analysis it was extracted from the spectrum and plotted as a function of pH. The observed variation with pH approximates a function describing the dissociation of a monobasic acid with a pKa of around 6, which is close to the values determined for His17 and His32. The contributions of Tyr16, Phe10 and Phe34 to the near-UV CD spectrum were difficult to detect in the presence of the strong CD bands of the structurally well-defined Trp13.

Binding of the hydrophobic fluorescent dye ANS is commonly used to discriminate molten globules from native

Figure 5

The CD spectrum of GTD-C at a peptide concentration of 150 μM in 50 mM phosphate buffer and pH 5.8 as a function of temperature. **(a)** The temperatures are from bottom to top 275K, 294K, 314K, 333K, 352K, 356K, 361K and 371K. An isodichroic point is observed close to 203 nm, suggesting a cooperative two-state helix-to-coil transition. **(b)** The mean residue ellipticity at 208 nm as a function of temperature. At 358K, the peptide is denatured irreversibly and precipitates. A β-sheet-type spectrum is formed with a minimum at 217 nm, which masks the temperature dependence of the mean residue ellipticity at 222 nm.

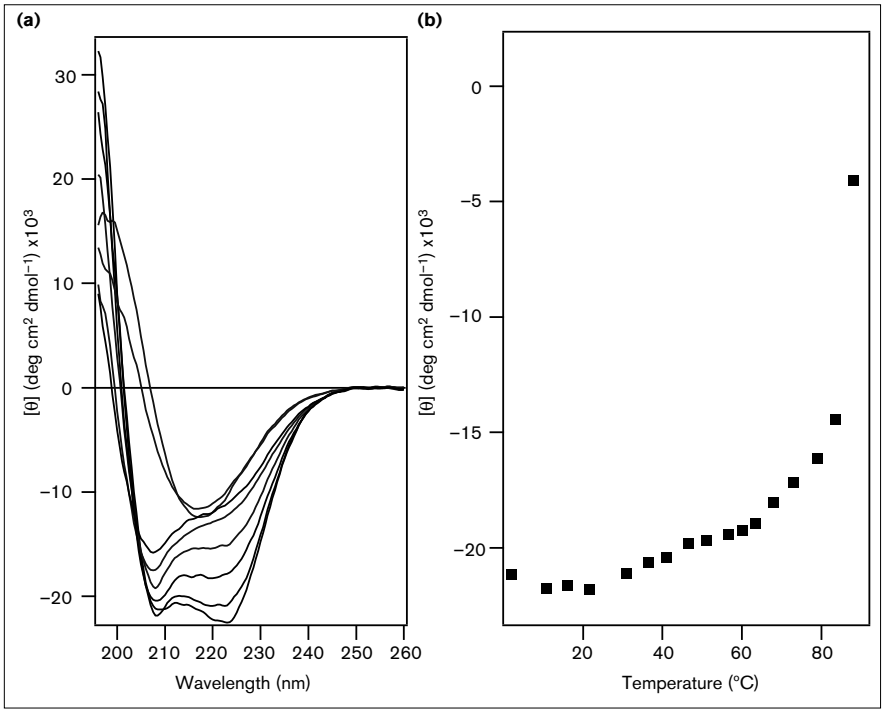

Figure 6

The near-UV CD spectrum of GTD-C at a peptide concentration of 330 μM in aqueous solution at 298K as a function of pH. **(a)** The near-UV CD spectrum at pH 4.1 (top trace) and at pH 8.4 (bottom trace). **(b)** The molar ellipticity of GTD-C at 272 nm as a function of pH. **(c)** The molar ellipticity of GTD-C at 293 nm as a function of pH. The molar ellipticity at 293 nm, i.e. the intensity of the ^1L_b vibronic band, becomes more negative with increasing pH. A function describing the dissociation of a monobasic acid with a pKa of 6.0 has been fitted to the experimental results.

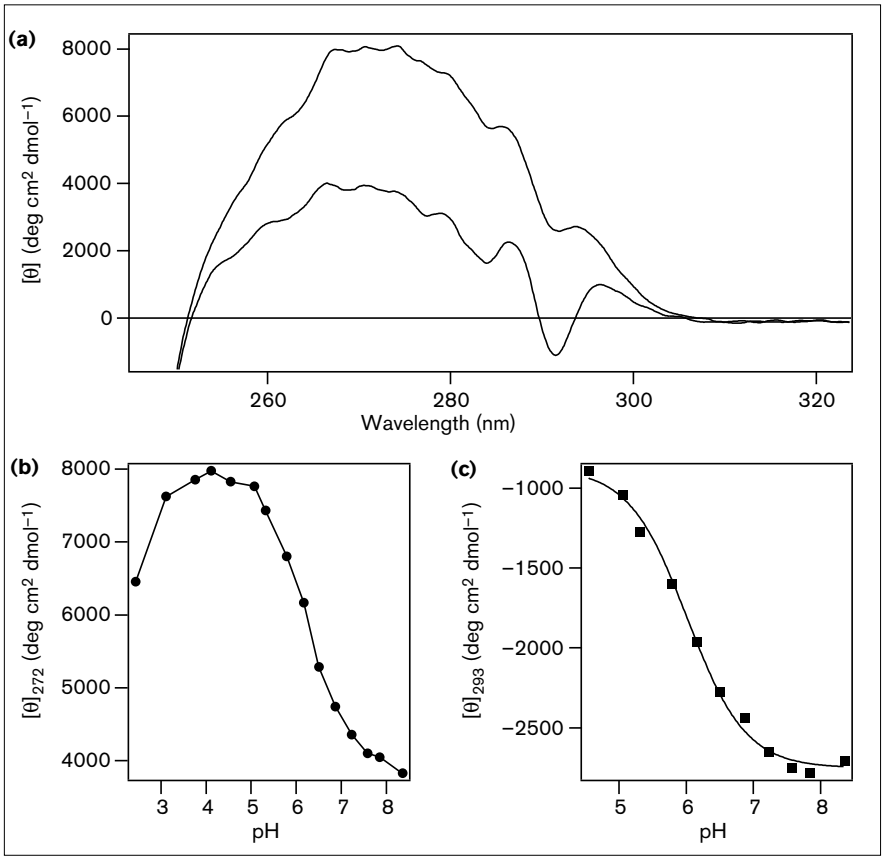

Figure 7

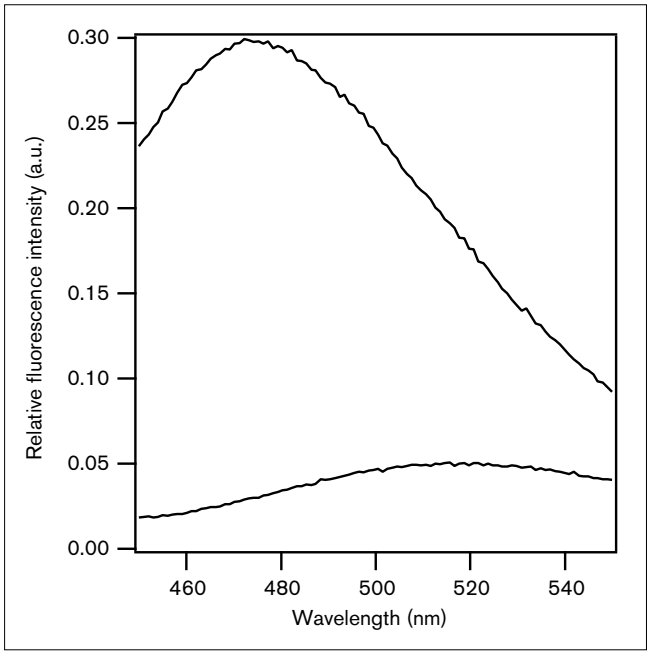

The emission spectrum of a 5 μM ANS solution (bottom trace) and of a 5 μM ANS solution containing 20 μM GTD-C (top trace), in 50 mM phosphate buffer at pH 5.8 and 293K, after excitation at 350 nm. The ANS fluorescence intensity is enhanced and the wavelength maximum is blue shifted due to ANS–peptide interactions. The emission spectrum of ANS in the presence of GTD-C has a maximum at 475 nm and its intensity is enhanced about six times.

Figure 8

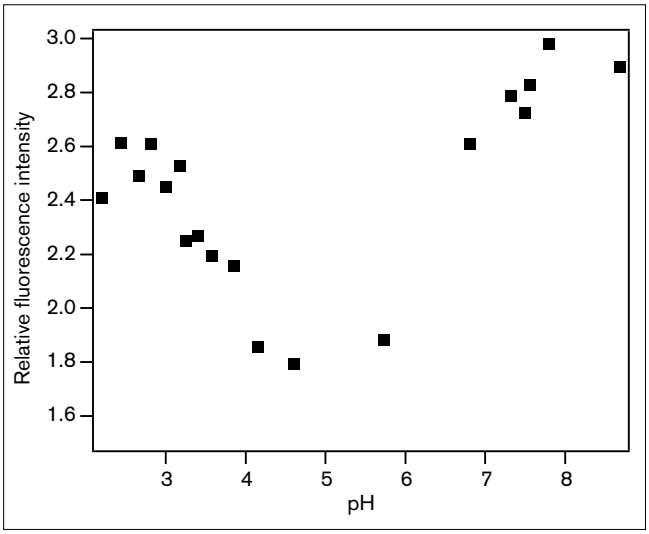

The fluorescence intensity of 20 μM ANS in the presence of 20 μM GTD-C in aqueous solution at 293K as a function of pH after excitation at 350 nm.

proteins [22]. ANS is not expected to bind to proteins with well-defined tertiary structures nor to random coils, although binding to native proteins has been observed. ANS is, however, known to have a strong affinity for molten globule states. The binding of ANS to a protein is accompanied by enhanced fluorescence intensity and a blue shift of the fluorescence maximum wavelength. GTD-C binds ANS, and the fluorescence spectra of free ANS and of ANS interacting with GTD-C at pH 5.8 are shown in Figure 7. The addition of 20 μM peptide to a solution of 5 μM ANS at pH 5.8 increases the ANS fluorescence intensity by a factor of only 6, which is very little since the intrinsic fluorescence of ANS is often plotted as the baseline in similar experiments. The binding is weak and no curvature is observed in the plot of fluorescence intensity versus concentration of ANS in the range 0 to 200 μM for a peptide concentration of 50 μM. The dissociation constant for the peptide–ANS complex cannot be determined since the errors due to the inner filter effect are too large at the concentrations of ANS needed to obtain sufficient complexation.

The pH dependence of ANS binding of GTD-C has instead been monitored by recording the fluorescence spectrum of ANS in a solution containing 20 μM peptide and 20 μM ANS as a function of pH (Figure 8). At a pH below 3, where GTD-C has a low helical content, weak peptide interactions with ANS are observed. In the pH interval between 3 and 4, the helix content increases and ANS fluorescence is at a maximum. At pH 5, the weakest ANS fluorescence is observed and the peptide–ANS interactions are weak, probably due to the formation of a well-defined tertiary structure of GTD-C. At pH 7.5, the most intense fluorescence is observed, which suggests the formation of a molten globule state, and above pH 7.5, the ANS fluorescence again decreases although the helical content is as high as at pH 5.

The pKa values of His17 and Asp27

The pKa values of the two histidine residues were determined by measuring the chemical shifts of the ring protons as a function of pH* (uncorrected) in D_2O solution at 288K. Below pH 3, where the helical content is low, the downfield ring protons of both histidine residues are sharp, but at pH 4.2, where the structure is approaching optimum conformational stability, one of them is severely broadened in spite of the fact that it is more than 99% protonated.

Differential broadening of the resonances of the two histidines is clearly observed until a pH of 5.9 has been reached, but at higher pH they overlap and separate linewidths cannot be estimated. The upfield His ring-proton resonances overlap with the aromatic protons of Trp, Phe and Tyr and can be observed only in the difference spectrum, where broadening is also observed for one of the resonances. The broadened resonances were

tentatively assigned as those of His17, due to the fact that the resonances of His17 in GTD-43, too, were broadened. Selective broadening of the resonances of one His residue may arise due to participation in a salt bridge and restricted conformational freedom. His32 was incorporated on the surface of the folded motif and was therefore expected to be more mobile and have sharper resonances. The pKa values are almost the same and a pKa of 6.5 was measured for the broadened resonances and tentatively assigned to His17 and a pKa of 6.4 was measured and assigned to His32. The expected value for a solvent exposed His residue is 6.4 [23].

The pKa of Asp27 is expected to be 4.0 from the determination of the pKa of Asp sidechains in model peptides. The chemical shifts of Asp27 have not yet been assigned, but a residue with the spin system of an aspartic acid, one α and two β protons, and chemical shifts that are close to those of Asp27 in GTD-43 titrates in a way that is compatible with a pKa of approximately 4. The simultaneous concentration of unprotonated Asp and protonated His should therefore have a rather shallow maximum centered at pH 5. An accurate determination of the pKa of Asp27 is not possible due to the documented structural changes of GTD-C that occur at low pH so that the measured chemical shifts do not reflect the state of protonation alone. The pKa value of Asp27 can therefore deviate significantly from the value of 4.

The free energy of unfolding of GTD-C

The Gibbs free energy of unfolding of GTD-C was determined by GuHCl and urea denaturation by monitoring the mean residue ellipticity at 222 nm, as a function of denaturant concentration at 298K and pH 5.8 [24] (Figure 9). Under the assumption that the concentration of the folded monomer is negligible, the denaturation may be described by a two-state model including only folded dimers (F_2) and unfolded monomers (U) [25].

$$F_2 \overset{K_U}{\rightleftharpoons} 2U \tag{1}$$

$$K_U = \frac{[U]^2}{[F_2]} = 2P_t\left(\frac{f_U^2}{1-f_U}\right) \tag{2}$$

K_U is the dissociation constant, P_t is the total peptide concentration and f_U is the molar fraction of unfolded peptide as described by equation 3:

$$f_U = \frac{(\theta_F - \theta_{obs})}{(\theta_F - \theta_U)} \tag{3}$$

where θ_{obs} is the observed ellipticity at 222 nm and θ_F and θ_U are the ellipticities at 222 nm of the folded and unfolded states, respectively. The mean residue ellipticities of the folded and unfolded states vary with the concentration of denaturant and, as a result, slopes are observed outside the transition region that are usually taken into account in the determination of the equilibrium constants [26]. θ_F and θ_U are given by equations 4 and 5:

$$\theta_F = \theta_F^{H_2O} + m_F[D] \tag{4}$$

$$\theta_U = \theta_U^{H_2O} + m_U[D] \tag{5}$$

$\theta_F^{H_2O}$ and $\theta_U^{H_2O}$ are the ellipticities in aqueous solution obtained as the intercepts at zero denaturant concentration, m_F and m_U are the slopes of the baselines, and D is the denaturant. The free energy of unfolding, ΔG_{obs}, is calculated for each denaturant concentration as $-RT \ln K_U$, and the Gibbs free energy of unfolding in aqueous solution, ΔG^{H_2O}, is estimated by linear extrapolation to zero denaturant concentration, as described in equation 6:

$$\Delta G_{obs} = \Delta G_{FU}^{H_2O} + m_{FU}[D] \tag{6}$$

The combination of equations 2–6 and $\Delta G_{obs} = -RT \ln K_U$ leads to equation 7, where θ_{obs} is given as a function of denaturant concentration, [D]:

Figure 9

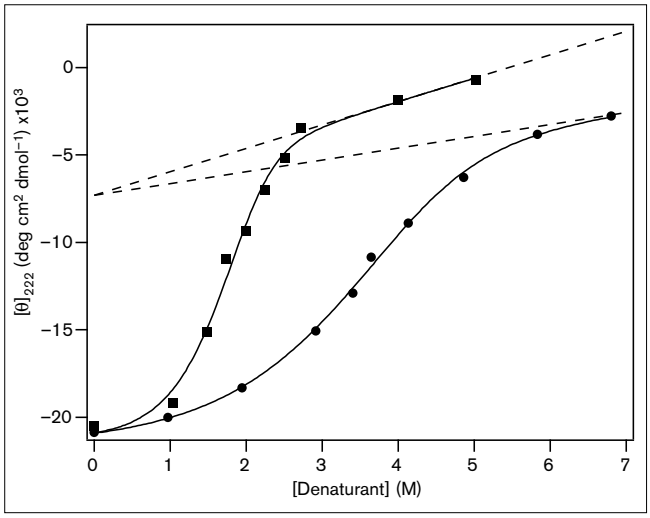

The mean residue ellipticity at 222 nm of GTD-C as a function of GuHCl (filled squares) and urea (filled circles) at pH 5.8 and 298K. The solid lines show the nonlinear least-squares best fits of equation 7 to the experimental results. The dotted line that describes the dependence of the mean residue ellipticity of the denatured peptide on GuHCl concentration was calculated from equation 5 using parameters obtained from the least-squares fit and the value of the intercept obtained from the GuHCl denaturation was used in the calculation of the corresponding function for urea denaturation. The slopes of the corresponding functions for the folded peptide could not be determined from the experimental results and were set to 0. The resulting free energy of unfolding for GuHCl is 9.7 kcal mol^{-1} and for urea it is 9.0 kcal mol^{-1}.

$$\theta_{obs} = \theta_F^{H_2O} + m_F[D] + \left\{\theta_U^{H_2O} + m_U[D] - \theta_F^{H_2O} - m_F[D]\right\} * \left\{-\left[\exp-\left(\left(\Delta G^{H_2O} + m_{FU}[D]\right)/RT\right)\right]/4P_t \pm \sqrt{\left(\left[\exp-\left(\left(\Delta G^{H_2O} + m_{FU}[D]\right)/RT\right)\right]4P_t\right)^2 + \left[\exp-\left(\left(\Delta G^{H_2O} + m_{FU}[D]\right)/RT\right)\right]}/2P_t\right\} \quad (7)$$

Nonlinear least-squares fitting of equation 7 to the experimental results gives the free energy of unfolding in aqueous solution. For GTD-C at pH 5.8 and 298K, it is 9.7 ± 0.6 kcal mol^{-1} for GuHCl denaturation and 9.0 ± 0.3 kcal mol^{-1} for urea denaturation. The concentration of GuHCl required to reduce the helical content of GTD-C to 50% was 2.0 M and the required concentration of urea was 3.8 M.

Trifluoroethanol (TFE) is a solvent that disrupts quaternary and tertiary protein structures and stabilises single-stranded α-helices in sequences with α-helical propensity. The effect of TFE on the CD spectrum of GTD-C is shown in Figure 10. The absolute value of the mean residue ellipticity at 222 nm does not increase on addition of TFE and the helical segments are therefore fully developed already in aqueous solution. The ratio $\theta_{222}/\theta_{208}$ is 0.99 in aqueous solution at pH 5.8, but decreases with increased TFE concentration to reach a value of 0.8 at 50 vol % TFE. The change of the ratio of $\theta_{222}/\theta_{208}$ is due only to the variation in θ_{208}, since θ_{222} does not change with TFE, and the ratio was therefore used for the study of TFE denaturation in a manner that was analogous to the way in which θ_{222} was used for the study of GuHCl and urea denaturation.

If it is assumed that the equilibrium between folded tertiary structure (T_2) and single-stranded α-helices (H) can be described by a two-state model, the dissociation constant, K_{PU}, is given by:

$$T_2 \overset{K_{PU}}{\rightleftharpoons} 2H \quad (8)$$

$$K_{PU} = \frac{[H]^2}{[T_2]} = 2P_t\left(\frac{f_H^2}{1-f_H}\right) \quad (9)$$

P_t is the total peptide concentration and f_H is the molar fraction of single-stranded helical states as described by:

$$f_H = \frac{(r_F - r_{obs})}{(r_F - r_U)} \quad (10)$$

where r_{obs} is the observed ratio $\theta_{222}/\theta_{208}$ and r_F and r_U are the ratios of the folded and single-stranded α-helical states, respectively. The assumption that the dissociation can be described by a two-state model is supported to some extent by the fact that θ_{222} is unaffected by TFE, which shows that the helical structures are approximately the same in TFE as they are in the folded dimer. This does not mean to imply that the unfolded monomers in aqueous solution are the same as those in TFE. The free energy associated with the formation of helical monomers, ΔG_{PU}, is $-RT \ln K_{PU}$. The value of the Gibbs free energy in aqueous solution, $\Delta G_{PU}^{H_2O}$ is estimated by linear extrapolation to zero TFE concentration. The calculated free energy associated with the formation of single-stranded α-helices from the four-helix bundle at 298K is 7.5 kcal mol^{-1}.

The reactivity of GTD-C

The reaction of GTD-C with mono-*p*-nitrophenyl fumarate was studied at pH 5.85 and 290K, and the second-order rate constant for the release of *p*-nitrophenol was $3.8 \pm 0.2 * 10^{-2}$ s^{-1} M^{-1}, which is comparable to that reported for RA-42, a helix–loop–helix dimer with ornithine as the flanking sidechain, $5.1 \pm 0.1 * 10^{-2}$ s^{-1} M^{-1} [14].

Figure 10

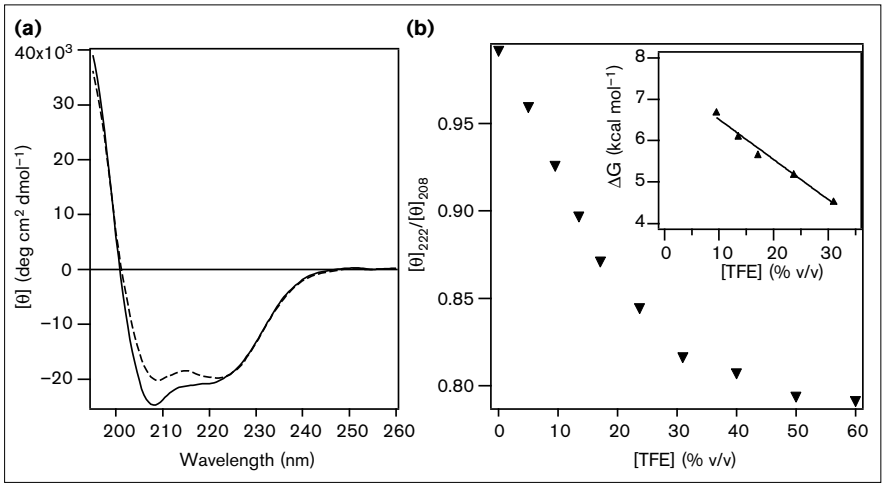

The effect of TFE on the CD spectrum of GTD-C at a peptide concentration of 38 μM in 50 mM phosphate buffer at pH 5.8 and 297K. **(a)** The CD spectrum of GTD-C at 0% (top trace) and 31% (v/v) (bottom trace) of TFE. The effect of TFE on the mean residue ellipticity at 222 nm is very small. **(b)** The ratio of mean residue ellipticities of GTD-C at 222 nm and 208 nm, $\theta_{222}/\theta_{208}$, as a function of TFE concentration. Inset: TFE denaturation of GTD-C as a function of TFE concentration. The intercept at zero TFE concentration is 7.5 kcal mol^{-1}.

Discussion

The structure of GTD-C

The structure of GTD-43 has been determined previously by NMR and CD spectroscopy and ultracentrifugation and it folds into a hairpin helix–loop–helix motif that dimerises to form a four-helix bundle [7,8]. The incorporation of His32, Lys36 and Glu3 to form GTD-C does not decrease the helical content; the mean residue ellipticity of GTD-C is –20,500 deg cm^2 $dmol^{-1}$, which is the same (within experimental error) as that of GTD-43. The mean residue ellipticity at 222 nm of GTD-C is concentration independent for total peptide concentrations in the range 3.8 to 760 μM and a concentration-independent CD spectrum was also found for GTD-43 where no decrease in helical content could be observed for concentrations as low as 4 μM. The free energy of unfolding for GTD-C determined by GuHCl is 9.7 ± 0.6 kcal mol^{-1}, which is the same within experimental error as that of GTD-43 (10.1 kcal mol^{-1}). Apparently the tertiary structure is unaffected by the changes in the amino acid sequence.

Further evidence for the formation of a well-developed structure in aqueous solution comes from the observation of a TFE-independent mean residue ellipticity and a blue-shifted Trp fluorescence maximum. The former observation shows that the helices are fully developed and the latter shows that the Trp is at least partly buried in the folded dimer.

GTD-C has a well-defined tertiary structure

The ^{1}H NMR spectrum of GTD-C at pH 4.5 and 283K is well dispersed, the NH chemical shifts cover a range of 2.29 ppm and the methyl region is 0.84 ppm. The corresponding shift ranges are 2.63 ppm and 0.94 ppm for IL-4, a naturally occurring four-helix bundle with 133 residues, and 2.14 ppm and 0.85 ppm for GTD-43 at pH 3.0 and 288K. The methyl region chemical shift dispersion is 0.75 ppm for α_2D but the NH dispersion has not yet been reported. Typical values for molten globules are 1.12 ppm and 0.15 ppm. The chemical shift dispersion of GTD-C is clearly comparable to that of IL-4, particularly in view of the fact that IL-4 has many more residues and longer loops that contribute to the dispersion because of the differences in secondary structure.

The temperature dependence of the ^{1}H NMR spectrum of GTD-C at pH 4.5 shows that the resolution is reduced with increased temperature due to line broadening, which is the expected behaviour for conformational exchange that is slow on the NMR timescale. In particular, the resonances in the amide and methyl regions become much better resolved at 283K than at higher temperatures.

The thermal denaturation of GTD-C was difficult to follow due to its precipitation at high temperature and irreversible attachment to the cuvette wall. The precipitation can be estimated from comparisons with other designed four-helix bundles to occur when the denaturation is past its midpoint but the contribution to the observed mean residue ellipticity at 222 nm by the glass-bound peptide is difficult to evaluate. The contribution to the CD spectrum is large and negative at 222 nm but close to zero at 208 nm and the thermal denaturation was therefore investigated by following the mean residue ellipticity at 208 nm as a function of temperature. The estimated temperature interval for thermal denaturation is about 30K.

In addition, the near-UV CD spectrum of GTD-C at pH 4.5 shows fine structure that is unusual for designed proteins and suggests that the Trp residue is located in an ordered environment. The aromatic ensemble consisting of Phe10, Trp13 and Phe34 has been shown previously to form a well-ordered structure in GTD-43 and it apparently remains so in the hydrophobic core of GTD-C.

The chemical shift dispersion and temperature dependence of the ^{1}H NMR spectrum of GTD-C, the narrow temperature interval for thermal denaturation and the appearance of the near-UV CD spectrum of GTD-C show that it has a well-defined tertiary structure.

The pH dependence of the tertiary structure of GTD-C follows the putative formation of an interhelical hydrogen-bonded ion pair between the ionized forms of His17 and Asp26

The resolution of the ^{1}H NMR spectrum, the mean residue ellipticity at 222 nm, the ratio of mean residue ellipticities, $\theta_{222}/\theta_{208}$, the intensities of the near-UV CD ^1L_a bands and the ANS binding show a strong dependence on pH. The probes that are commonly used to identify conformational stability, i.e. the ^{1}H NMR spectrum, ANS binding and the intensities of the strong near-UV CD bands, all have optima centered around pH 5. In addition, the ratio of mean residue ellipticities has a broad maximum with a value that is close to 1 centered around pH 5, which suggests that the formation of the coiled-coil motif is optimal in the same region. The formation of a well-defined tertiary structure therefore has a pH optimum that is centered around pH 5 and the structure is severely degraded upon titration to low and to high pH from that of the optimum conformation.

The observation of a pronounced pH optimum must be linked to the ionization of more than one residue, one of which should have a pKa of approximately 6.5 and the other should have a pKa that is slightly less than 4. The measured pKa values for both histidines are 6.5 within experimental error and no other residues are expected to have dissociation constants that fit the observed pH dependence. His32 is located on the surface of the folded peptide as demonstrated by its reactivity towards mono-*p*-nitrophenyl fumarate. The release of *p*-nitrophenol with the second-order rate constant that was measured for

Figure 11

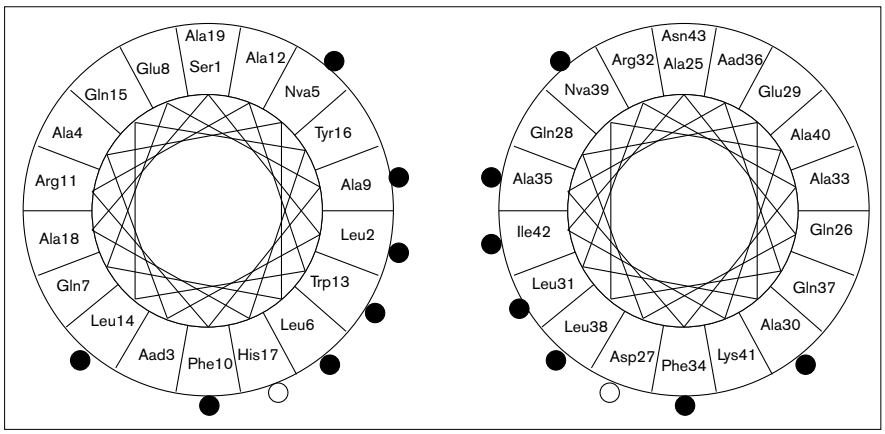

Helical wheel representation of the designed helices in GTD-C showing the putative formation of a salt bridge between HisH17^{+} and Asp27^{-}.

GTD-C occurs only for histidine residues that are flanked by lysine or arginine residues in positions *i*,*i*+4, *i*,*i*+3 or *i*,*i*–3 [14] and this condition is fulfilled only for the His32 Lys36 pair. Consequently, His32 is located on the surface of the folded peptide and can stabilise only the folded helix, which is not sufficient to provide conformational stability for the tertiary structure. His17, on the other hand, is located in the interior of the four-helix bundle as it flanks Trp13 in helix I and the observed pH dependence is therefore most likely due to the dissociation of HisH17^{+} (Figure 11).

A pKa of 4 cannot be determined in GTD-C because the tertiary structure is disrupted at low pH and the chemical shifts cannot be assumed to be due to the state of protonation alone. The pKa values must therefore be estimated from those of model peptides where the pH of the sidechain of Asp is 4.0 and that of Glu is 4.5. The observed pH dependence fits the expected deprotonation of Asp27, which is the only Asp in the sequence, although the possibility of a Glu with a depressed pKa or a general field effect from the simultaneous deprotonation of many carboxylic acids cannot be excluded.

His17 is close to Asp27 in the folded hairpin motif and the formation of an interhelical salt bridge fits the observed pH dependence very well, particularly if the pKa of Asp is a few tenths of a unit below 4.0. The observation that a well-defined tertiary structure is formed is also in agreement with the formation of a salt bridge between His17 and Asp27. The effect of forming a hydrogen-bonded ion pair would be to reduce the degrees of freedom of the helices, which is the designed function of a conformational constraint.

The free energy of unfolding of GTD-C at pH 5.8 is the same as that of GTD-43 at pH 3.0

The putative salt bridge between His17 and Asp27 is not strictly internal as it is located at the boundary between the hydrophobic core and the loop region, and complete desolvation of the charged groups is not necessary for its formation. Thermodynamically, it would not be expected to provide much net binding energy over that provided by complementary hydrophobic residues. The favourable contribution by salt bridges has been shown to roughly cancel out the negative contribution from desolvation of the charged groups and hydrophobic interactions can provide much binding energy. In the Arc repressor of bacteriophage P22, it was demonstrated that the thermodynamic stability was in fact increased by replacing the internal salt bridge by complementary hydrophobic residues. The reason for the improved conformational stability of GTD-C in comparison with those of most *de novo* designed proteins is therefore not the increased binding energy per se, but the increase in free energy that results from deviating from optimum geometry since this leads to 'unpaired' charged residues in a hydrophobic environment. The thermodynamic cost or gain of forming a salt bridge has been investigated by measuring the free energy of unfolding of GTD-43 at a pH where there is little salt bridge formation and that of GTD-C at a pH where there is substantial salt bridge formation. The net difference in helix propensity between the amino acid residues His and Lys in GTD-C and Arg and Aad (Glu) in GTD-43 is small since His has a lower helix propensity than Arg but Aad (Glu) has a lower propensity than Lys [1]. The free energy of unfolding of GTD-C at pH 5.8 is 9.7 kcal mol^{-1}, which is the same (within experimental error) as that of GTD-43 at pH 3.0 (10.1 kcal mol^{-1}). Consequently, in GTD-C the His17 Asp27 ion pair contributes little to the overall thermodynamic stability of the folded dimer but the gain in conformational stability is striking. The incorporation of interhelical salt bridges in designed proteins where the thermodynamic stability is sufficient may therefore be of general use in *de novo* design of proteins with well-defined tertiary structures. The interesting issue of what properties are found in GTD-C when the salt bridge is replaced by two hydrophobic residues, however,

remains to be resolved. Those experiments are now in progress in our laboratory.

Cooperativity in the folding of GTD-C

The observation of an isodichroic point in the thermal denaturation of GTD-C suggests that the transition from coil to helix is cooperative and may be described by a two-state model. The free energy of unfolding is a measure of the transition from coil to folded structure and it has been measured by GuHCl as well as by urea denaturation and found to be 9.7 kcal mol^{-1} and 9.0 kcal mol^{-1}, respectively. TFE has been used to denature proteins and to force the formation of helical structures in sequences with helical propensity. The effect of TFE on the structure of the folded dimer of GTD-C is only to disrupt the tertiary structure to form non-hairpin helix–loop–helix monomers, since the helical content is unaffected by the solvent. Since the free energy of unfolding by GuHCl measures the disruption of the folded dimers and the formation of coil-like structures, whereas that by TFE measures only the disruption of the folded dimers, a comparison of the two numbers should provide information on the degree of cooperativity. The application of the corresponding equations to the TFE denaturation process as used for GuHCl denaturation leads to a free energy of unfolding for TFE denaturation of 7.5 kcal mol^{-1}. The difference between 7.5 kcal mol^{-1} and 9.7 and 9.0 kcal mol^{-1} suggests that about 2 kcal mol^{-1} of folding energy is provided by the helix propensity of the two helices and that intermediate structures may be populated in the folding process.

Conclusions

The engineering of an interhelical salt bridge has been strongly suggested by the pH dependence of a number of spectroscopic probes to induce conformational stability in a designed helix–loop–helix motif, i.e. it introduces specificity in helix–helix recognition. The hydrogen-bonded ion pair provides little thermodynamic stability over that of the non-hydrogen-bonded ion pair in agreement with previously reported studies on proteins, but the effects on the tertiary structure of the folded peptide are striking. The combined use of interhelical salt bridges and shape-complementary hydrophobic interfaces therefore appears to be a design principle of general use in the *de novo* design of proteins with well-defined tertiary structures.

Materials and methods

Synthesis, purification and identification of GTD-C

GTD-C was synthesised on a Biosearch 9600 automated peptide synthesiser using general Fmoc procedures on a 0.16 mmol scale using a PAC-PEG linked Asn(Trt) polymer (PerSeptive Biosystems). The sidechains were protected with the piperidine-stable Pmc (Arg), Trt (Asn, Gln and His), OtBu (Asp and Glu), Boc (Lys and Trp) and tBu (Ser, Thr and Tyr) groups and the Fmoc group was removed by 30% piperidine in DMF (v/v). Fmoc-protected amino acids (4 equiv) were coupled to the growing peptide chain for 2 h in 6 ml NMP with TBTU:HOBt:DIPEA (1:1:1; 4 equiv) as coupling reagent in the first coupling step. Amino acids for which a second coupling with fresh reagents was required were allowed to react for an additional 2 h using DCM:DMF:NMP (1:1:1; v/v) with 1% Triton X100 as the solvent using the same coupling reagent as in the first coupling step. In the synthesis of the template polypeptide, GTD-43, it was found after analysis of the reaction products by MALDI MS that in the sequence from Ala33 to Pro24 the coupling yields were not quantitative. The corresponding sequence in GTD-C was therefore double coupled. All couplings were performed at 28°C, by gentle heating of the reaction flask with a heating coil. The deprotection and cleavage from the resin of GTD-C was accomplished with a mixture of TFA:thioanisol:anisol:1,2-ethandithiol (90:5:3:2; v/v). A volume of 15 ml was used to cleave 1 g of polymer with stirring for 3.5 h at room temperature. After removing the resin by filtration, the peptide was precipitated by the addition of 200 ml of cold diethyl ether. The precipitate was washed three times with 100 ml cold diethyl ether, dried under vacuum and desalted on a Sephadex G25 column with 0.1% TFA as the eluent. The collected peptide fraction was lyophilised and stored below 0°C. GTD-C was purified by preparative high-pressure liquid chromatography on a reversed-phase Kromasil C-8 25×250 mm column with an isocratic mixture of 32% isopropanol and 0.1% TFA as eluent at a flow rate of 9 ml min^{-1}. The peptide eluted as a broad peak with a retention time of 39 min and was identified from its electrospray mass spectrum, recorded on a VG Analytical ZabSpec sector instrument (calculated 4721.1, found 4720.9).

NMR spectroscopy

500 MHz ^{1}H NMR spectra were recorded on a Varian Unity 500 NMR spectrometer equipped with a matrix shim system from Resonance Research Inc. using a 90° pulse of 8.9 μs and a sweep width of 7000 Hz. Solvent suppression was accomplished by weak pre-irradiation of the water resonance. The pKa values of the histidine residues were determined at 293K by measuring the chemical shifts of the ring protons in D_2O solution under the usual assumption that the isotope effects on pH* (uncorrected) and the dissociation constants cancel. The pH was adjusted with 0.1 M DCl and 0.1 M NaOD. The temperature dependence of the ^{1}H NMR spectrum of GTD-C was determined at pH 4.5. The chemical shift ranges of the NH and hydrophobic core methyl groups were measured from the TOCSY spectrum where the NH and methyl chemical shifts are easily identified from the observation of sidechain spin systems.

Circular dichroism spectroscopy

CD spectra were acquired with signal averaging on a Jasco J-720 spectropolarimeter and a baseline was recorded separately and subtracted. The instrument was routinely calibrated using d-10-(+)-camphorsulphonic acid. The spectra were processed and presented using the IGOR software from Wavemetrics Inc. Far-UV spectra were recorded from 260 to 185 nm, using quartz cells, 1 nm bandwidths and 0.25 s response times. The spectra are the average of at least four scans. Near-UV CD spectra were recorded from 350 to 240 nm, using a 0.5 cm quartz cell, 2 nm bandwidths and 1 s response times. The spectra are the averages of six scans. Far-UV ellipticities are reported as mean residue ellipticities, and near-UV ellipticities are reported as molar ellipticities per residue, using the molecular weight 4721.

Stock peptide concentrations were determined spectrophotometrically in 6.0 M GuHCl using an exctinction coefficient at 280 nm of 6756. The far-UV CD pH profile of GTD-C was recorded using a 61 μM peptide solution in aqueous solution at 298K and the near-UV CD pH profile was recorded using a 330 μM peptide solution in aqueous solution at 298K. The pH was adjusted with 0.1 M HCl and NaOH. The temperature dependence of the mean residue ellipticity of a 151 μM solution of GTD-C in 50 mM phosphate buffer pH 5.8 was recorded using a 0.5 mm thermostatted quartz cell connected to a circulating Lauda-T water bath in the temperature range 275–363K. The sample cell temperature was raised in 5° increments with 10 min equilibration times between spectra. The effect of TFE on the structure of GTD-C was determined using a 38 μM peptide solution in 50 mM phosphate buffer at pH 5.8 and 298K in the range from 0 to 60 vol % TFE (v/v).

The molar ellipticity was calculated with due consideration to the dilution of the sample by the addition of TFE.

Denaturation of GTD-C by 0–5 M GuHCl was carried out using a peptide concentration of 63 μM in 50 mM phosphate buffer at pH 5.8 and 298K. Samples were prepared from a 1.5 mM stock peptide solution, a stock 7.73 M GuHCl solution (7.73 M) and diluted to the final volume by the addition of buffer and equilibrated for 30 min before analysis. The concentration of the stock GuHCl solution was determined from its refractive index.

The denaturation of GTD-C by 0–7 M urea was carried out in the same way as by GuHCl but using a peptide concentration of 50 μM in 50 mM phosphate buffer at pH 5.8 and 298K. The samples were prepared from a 330 μM stock peptide solution, a 8.1 M stock urea solution and the sample was diluted to its final volume by buffer. The samples were equilibrated for 30 min before analysis. The concentration of the stock urea solution was determined from its refractive index.

Fluorescence measurements

Fluorescence spectra were recorded on a Spex 1680 Fluorolog τ2 spectrometer using a 1.0 cm reduced cell with a sample volume of 200 μl, 4 nm bandwidths and a 0.5 s response time. The baseline was recorded separately and subtracted from the spectra, which were also corrected for the inner filter effect. ANS fluorescence in the presence of 50 μM GTD-C at 288K was recorded in 50 mM phosphate buffer at pH 5.8 by titration with a mixture of 50 μM GTD-C and 400 μM ANS in 50 mM phosphate buffer at pH 5.8. The concentration of ANS was increased from 0 to 200 μM. ANS was excited at 350 nm and the emission was recorded at 1 nm intervals between 420 and 550 nm. ANS fluorescence as a function of pH in the presence of GTD-C was measured using an aqueous solution of 20 μM GTD-C and 20 μM ANS, which was titrated with 0.01 M HCl and 0.01 M NaOH. ANS was excited at 350 nm and the spectra were recorded between 400 and 600 nm at 293K. ANS was also excited by energy transfer from Trp13 which was excited at 295 nm and the spectra were then recorded between 300 and 600 nm at 293K.

Tryptophan fluorescence was recorded using a 23 μM aqueous peptide solution at pH 5.8 with and without 5 M GuHCl, with excitation at 280, 290 and 295 nm. The emission spectra were recorded at 1 nm intervals between 310 and 400 nm. Tryptophan fluorescence as a function of pH was recorded using a 20 μM aqueous GTD-C solution that was titrated with 0.01 M HCl and 0.01 M NaOH. The spectra were recorded at 293K between 300 and 400 nm with excitation at 295 nm.

Kinetics

The pseudo first-order rate constants for the reaction between GTD-C and mono-*p*-nitrophenyl fumarate in 50 mM Bis-Tris buffer at pH 5.8 and 290K were determined by following the release of *p*-nitrophenol at 320 nm. The second-order rate constant for the reaction was determined from the slope of the plot of the pseudo first-order rate constants versus concentration of peptide. The concentration of the substrate was 190 μM and that of the peptide was between 180 and 380 μM.

Acknowledgements

Financial support from Carl Tryggers Stiftelse and the Swedish Natural Science Research Council is gratefully acknowledged.

References

1. Bryson, J.W., *et al*., & DeGrado, W.F. (1995). Protein design: a hierarchic approach. *Science* **270,** 935-941.
2. Johnsson, K., Allemann, R.K., Widmer, H. & Benner, S.A. (1993). Synthesis, structure and activity of artificial, rationally designed catalytic polypeptides. *Nature* **365,** 530-532.
3. Kaumaya, P.T.P., Berndt, K.D., Heidorn, D.B., Trewhella, J., Kezdy, F.J. & Goldberg, E. (1990). Synthesis and biophysical characterization of engineered topographic immunogenic determinants with αα topology. *Biochemistry* **29,** 13-23.
4. Rabanal, F., DeGrado, W.F. & Dutton, P.L. (1996). Toward the synthesis of a photosynthetic reaction center maquette: a cofacial porphyrin pair assembled between two subunits of a synthetic four-helix bundle multiheme protein. *J. Am. Chem. Soc.* **118,** 473-474.
5. Dolgikh, D.A., *et al*., & Ptitsyn, O.B. (1985). Compact state of a protein molecule with pronounced small-scale mobility: bovine α-lactalbumin. *Eur. Biophys. J.* **13,** 109-121.
6. Raleigh, D.P., Betz, S.F. & DeGrado, W.F. (1995). A *de novo* designed protein mimics the native state of natural proteins. *J. Am. Chem. Soc.* **117,** 7558-7559.
7. Dolphin, G.T., Brive, L., Johansson, G. & Baltzer, L. (1996). Use of aromatic amino acids residues to restrict the dynamics in the hydrophobic core of a designed helix-loop-helix dimer. *J. Am. Chem. Soc.* **118,** 11297-11298.
8. Brive, L., Dolphin, G.T. & Baltzer, L. (1997). Structure and function of an aromatic ensemble that restricts the dynamics of the hydrophobic core of a designed helix-loop-helix dimer. *J. Am. Chem. Soc.* **119,** 8598-8607.
9. Struthers, M.D., Cheng, R.P. & Impeirali, B. (1996). Design of a monomeric 23-residue polypeptide with defined tertiary structure. *Science* **271,** 342-345.
10. Betz, S.F. & DeGrado, W.F. (1996). Controlling topology and native-like behavior of *de novo*-designed peptides: design and characterization of antiparallel four-stranded coiled coils. *Biochemistry* **35,** 6955-6962.
11. Handel, T.M., Williams, S.A. & DeGrado, W.F. (1993). Metal ion-dependent modulation of the dynamics of a designed protein. *Science* **261,** 879-885.
12. Waldburger, C.D., Schildbach, J.F. & Sauer, R.T. (1995). Are buried salt bridges important for protein stability and conformational specificity? *Nat. Struct. Biol.* **2,** 122-128.
13. Schneider, J.P., Lear, J.D. & DeGrado, W.F. (1997). A designed buried salt bridge in a heterodimeric coiled coil. *J. Am. Chem. Soc.* **119,** 5742-5743.
14. Baltzer, L., Lundh, A.-C., Broo, K., Olofsson, S. & Ahlberg, P. (1996). Polypeptides with supersecondary structures as templates in rational catalyst design. Catalysis of self functionalization by designed helix-loop-helix motifs. *J. Chem. Soc. Perkin Trans.* **2,** 1671-1676.
15. Lundh, A.-C., Broo, K. & Baltzer, L. (1997). The relationship between structure and reactivity in a designed helix-loop-helix motif. *J. Chem. Soc. Perkin Trans.* **2,** 209-212.
16. Zhou, N.E., Kay, C.M. & Hodges, R.S. (1994). The net energetic contribution of interhelical electrostatic attractions to coiled-coil stability. *Protein Eng.* **7,** 1365-1372.
17. Cooper, T.M. & Woody, R.W. (1990). The effect of conformation on the CD of interacting helices: a theoretical study of tropomyosin. *Biopolymers* **30,** 657-676.
18. Lakowicz, Y. (1983). *Principles of Fluorecence Spectroscopy.* Plenum Press, New York.
19. Steiner, R.F. & Kirby, E.P. (1969). The interaction of the ground state and excited states of indole derivatives with electron scavengers. *J. Phys. Chem.* **73,** 4130-4135.
20. Powers, R., Garret, D.S., March, C.J., Frieden, E.A., Gronenborn, A.M. & Clore, G.M. (1992). ^{1}H, ^{15}N, ^{13}C and ^{13}CO assignments of human interleukin-4 using three-dimenstional double- and triple-resonance heteronuclear magnetic resonance spectroscopy. *Biochemistry* **31,** 4334-4346.
21. Strickland, E.H. (1974). Aromatic contributions to circular dichroism spectra of proteins. *CRC Crit. Rev. Biochem.* **2,** 113-175.
22. Semisotnov, G.V., Rodionova, N.A., Razgulyaev, O.I., Uversky, V.N., Gripas, A.F. & Gilmanshin, R.I. (1991). Study of the "molten globule" intermediate state in protein folding by hydrophobic fluorescent probe. *Biopolymers* **31,** 119-128.
23. Tanford, C. (1962). The interpretation of hydrogen ion titration curves of proteins. *Adv. Protein Chem.* **17,** 69-161.
24. Pace, C.N. (1986). Determination and analysis of urea and guanidine hydrochloride denaturation curves. *Methods Enzymol.* **131,** 266-280.
25. DeFrancesco, R., Pastore, A., Vecchio, G. & Cortese, R. (1991). Circular dichroism study of the conformational stability of the dimerisation domain of transcription factor LFB1. *Biochemistry* **30,** 143-147.
26. Santoro, M.M. & Bolen, D.W. (1988). Unfolding free energy changes determined by the linear extrapolation method. 1. Unfolding of phenylmethanesulfonyl α-chymotrypsin using different denaturants. *Biochemistry* **27,** 8063-8068.